19th Australasian Fluid Mechanics Conference
Melbourne, Australia
8–11 December 2014

Instability in a Precessing Cylinder Flow

H. M. Blackburn[1], T. Albrecht[1], R. Manasseh[2], J. M. Lopez[3] and P. Meunier[4]

[1]Department of Mechanical and Aerospace Engineering
Monash University, Victoria 3800, Australia

[2]Department of Mechanical and Product Design Engineering
Swinburne University of Technology, Victoria 3122, Australia

[3]School of Mathematical and Statistical Sciences
Arizona State University, Tempe AZ, USA

[4]IRPHE, CNRS and Aix-Marseille Universitié, Marseille, France

Abstract

Direct numerical simulation (DNS) results for flow inside a spinning, precessing cylinder of fluid corresponding to a previous experimental study are presented and analysed in relation to experimental results and weakly nonlinear theory based on triad interaction of inviscid Kelvin modes. The simulation outcomes agree well with the experimental results both qualitatively and quantitatively, and additional processing reveals more in-depth support for the weakly nonlinear theory than could be demonstrated in the experiments. Additionally, numerical results provide meridional and azimuthal mean flow data.

Introduction

In rotating flows, conservation of angular momentum can lead to oscillatory behaviour; in a rotating frame of reference, this behaviour can be couched in terms of a balance between inertial and Coriolis forces. In cylindrical containers of rotating fluid, the (linear) inviscid eigenmodes (Kelvin modes) and resonant frequencies of this phenomenon are readily predicted [4]. Provided Reynolds numbers are sufficiently high, the inviscid Kelvin modes are a reasonable approximation to the set of viscous eigenmodes of the basic state of solid-body rotation. The simplest of these are relatively easy to excite and observe experimentally [3, 11].

Even with quite small disturbance amplitudes, a rich variety of more interesting behaviours have been observed experimentally, such as 'resonant collapse' which can produce disordered and/or turbulent states [9, 11]. However, prior to the onset of these complicated states, it is also possible to observe apparently structured motions, leading to conjecture that many of these phenomena arise through nonlinear interaction between vibration modes of the basic state. McEwan [12] speculated that the resonant collapse of inertia wave modes was caused by nonlinear interactions of triads of waves, since this mechanism was known to exist for ocean-surface and stratified waves. This is usually modelled by a weakly nonlinear approach in which the linear eigenmodes are given amplitudes that evolve nonlinearly. However, Manasseh [10] was unable to explain experimental observations of inertia wave breakdown by use of nonlinear triad theory alone. Experiments by Fultz, Malkus, McEwan and Kobine [3, 8, 11, 5] had all shown the presence of an azimuthal mean flow during excitation of inertia waves. The possibility that a mean flow could 'tune' or 'detune' the modes led to heuristic inclusion of a mean flow in a triad theory e.g. [6, 7]. Through careful experimental design, it is possible to precisely target particular combinations of modal resonances, especially if the Kelvin modes are assumed as a basis set. One such set of theoretical and experimental investigations [6, 7, 13] forms the basis of the numerical modelling work that we describe below.

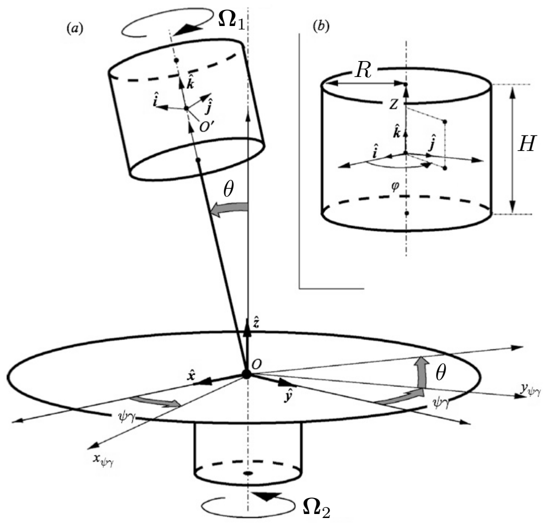

Figure 1: Schematic of experiment. Turntable rotates at rate Ω_2, cylinder of fluid rotates relative to turntable at rate Ω_1. After solid body rotation of fluid in cylinder is achieved, nutation angle θ rises from zero to a fixed maximum value.

The experimental setup is illustrated in figure 1: a cylinder of fluid, height H and radius R, spins about its axis at one rotation rate Ω_1 relative to a turntable with rotation rate Ω_2. After solid body rotation is achieved inside the cylinder, its axis is tilted through angle θ. For tuned rotation rate pairs, weakly nonlinear theory ([6], valid for small nutation angles) predicts an instability mechanism based on a coupling of Kelvin modes.

In the case principally considered here, $\theta_{\max} = 1^\circ$, $\Omega_1 = 1.18$, $\Omega_2 = -0.18$ and $Re = (\Omega_1 + \Omega_2 \cos\theta)R^2/\nu = 6500$, while the Rossby number $Ro = \Omega_2 \sin\theta/(\Omega_1 + \Omega_2 \cos\theta) = -0.0031$. The cylinder aspect ratio was chosen as $H/R = 1.62$, which is tuned to excite a weakly nonlinear resonance between the primary driven Kelvin mode with azimuthal wavenumber $m = 1$ and two other modes which have azimuthal wavenumbers $m = 5$ and 6 (radial and axial structures discussed below), as outlined in [6].

Computational method

We use a cylindrical-coordinate formulation of a nodal spectral element–Fourier method for the incompressible Navier–Stokes equations [2], expanded to solve in a reference frame rotating at angular velocity $\boldsymbol{\Omega} = \boldsymbol{\Omega}_1 + \boldsymbol{\Omega}_2$. Thus the equation set for solu-

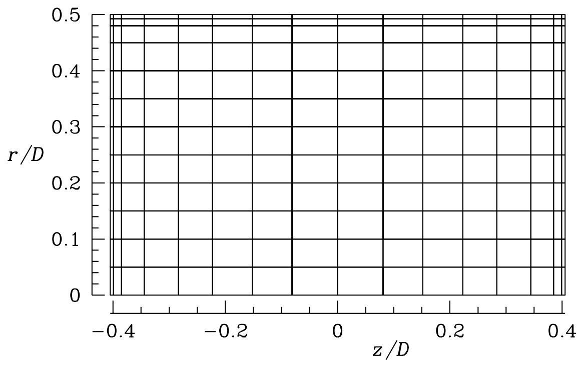

Figure 2: Spectral element mesh of the meridional semi-plane for a cylinder of height:radius ratio $H/R = 1.62$.

tion (steady and dynamically insignficant centrifugal terms can be expressed as the gradient of a scalar and so may be absorbed into the pressure term) is

$$\partial_t \boldsymbol{u} + \boldsymbol{u}\cdot\boldsymbol{\nabla}\boldsymbol{u} + 2\boldsymbol{\Omega}\times\boldsymbol{u} + \mathrm{d}\boldsymbol{\Omega}/\mathrm{d}t\times\boldsymbol{x} = \rho^{-1}\boldsymbol{\nabla}p + \nu\nabla^2\boldsymbol{u}, \quad (1)$$

$$\boldsymbol{\nabla}\cdot\boldsymbol{u} = 0, \quad (2)$$

and the mesh remains fixed. Since the angular velocity $\boldsymbol{\Omega}$ is the vector sum of the turntable and cylinder motor rotations, we can choose to solve either in a frame of reference aligned with the cylinder axis (where the cylinder rotates in it, so the cylinder walls move with respect to the reference frame), or in a frame of reference fixed to the cylinder, such that the walls appear fixed. A useful implementation check is that the flow dynamics should be identical, modulo a solid-body rotation, regardless of which choice is taken; we confirm that this is indeed the case for our code. The results presented below were computed in the cylinder axis frame of reference, so the initial basic state is solid-body rotation.

The mesh has 192 spectral elements covering the meridional semi-plane, as shown in figure 2, and 128 data planes (64 Fourier modes) in azimuth. Local mesh refinement is concentrated near the walls to resolve boundary-layer structure. Sixth-order tensor-product nodal basis functions are used in each element, giving at total of 7081 independent mesh nodes for each data plane and 906 368 nodes in total. We have checked this resolution is adequate to resolve flows for the parameters employed.

Dynamical behaviour

The initial state is solid-body rotation, representing steady-state flow in the cylinder with $\theta = 0$. The simulation is then initiated with a smooth (cosine-taper top-hat profile) increase in θ up to $\theta_{\max} = 1^\circ$ over 1/10th of a cylinder rotation period, i.e. over $0.1T$ where $T = 2\pi/\Omega_1$.

The dynamics of the flow are illustrated in figure 3, which shows the evolution of flow kinetic energy density partitioned into the 64 azimuthal Fourier modes included in the simulation. The dominant energy resides at $m = 0$, which is dominated by (axisymmetric) solid-body rotation. Within of order 20 cylinder rotation periods, the flow settles to a quasi-steady three-dimensional state with the non-axisymmetric component dominated by Fourier mode $m = 1$ (driven directly by the precession at frequency Ω_2 in $m = 1$) with higher modes directly slaved to Fourier mode pair $m = 0, 1$ through nonlinear coupling.

Soon after $100T$, an instability can be observed. Kinetic energies in Fourier modes $m = 5$ and $m = 6$ rise above their quasi-steady values, with an initial phase of linear growth lasting until approximately $170T$ when nonlinear saturation sets in with a corresponding drain of energy from Fourier mode $m = 1$. This triadic interaction ($m = 1, 5, 6$) is in good agreement with the predictions of weakly nonlinear theory as outlined in references [6, 13].

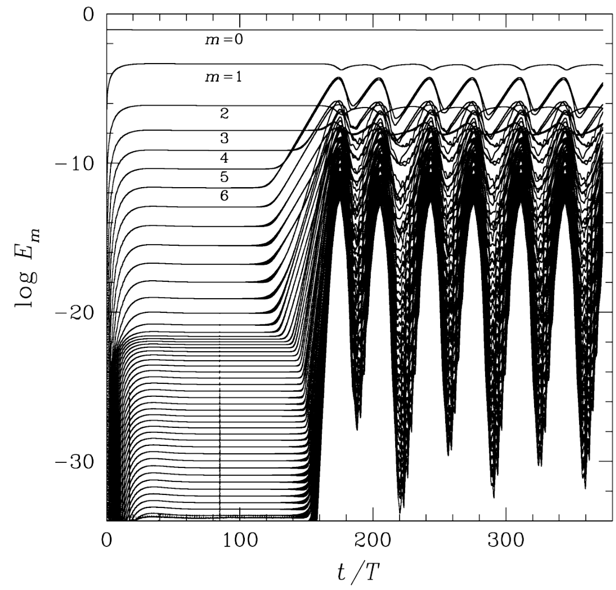

Figure 3: Temporal dynamics of flow kinetic energy E partitioned into azimuthal Fourier modes (azimuthal wavenumber index m).

Following initial saturation, behaviour apparently approaches a limit-cycle state, with approximate period $T_{\text{avg}} = 34.6T$, with all non-axisymmetric modes participating. This large-timescale behaviour is observed experimentally, and is also predicted by a refined weakly nonlinear theory, as set out in [7]. We note that such large-timescale quasi-periodicity has also been observed in earlier experiments, e.g. for breakdown types C and G of [9].

Each cycle contains a phase where azimuthal modes $m = 5$ and 6 grow exponentially by approximately two orders of magnitude before saturation and collapse. Their growth occurs at the expense of energy in $m = 1$. Again, these features — the azimuthal wavenumbers participating, and exponential growth — lend support to the idea that a weakly nonlinear interaction drives the instability.

Spatial structure

An examination of spatial structure on the cylinder mid-plane at a time when three-dimensional features were most evident was presented by Lagrange *et al.* [6, Fig. 2]. Their data were obtained via particle image velocimetry, using laser sheet lighting in a plane normal to the turntable axis, at cylinder mid-height ($z = 0$). We note that the background solid-body rotation was subtracted from the data prior to post-processing to obtain estimates of axial vorticity as reproduced here in figure 4 (a) — also that owing to practical restrictions, they were unable to resolve near-wall boundary layer structure. Azimuthal structures dominated by $m = 6$ are clearly seen. For comparison we show in figure 4 (b) an equivalent data extraction from our DNS for a time of approximately $340T$. This also shows dominance by $m = 6$ at this location, and also evidence of boundary layer structure near the cylinder walls that could not be resolved in experimental PIV measurements. Weakly nonlinear theory [6]

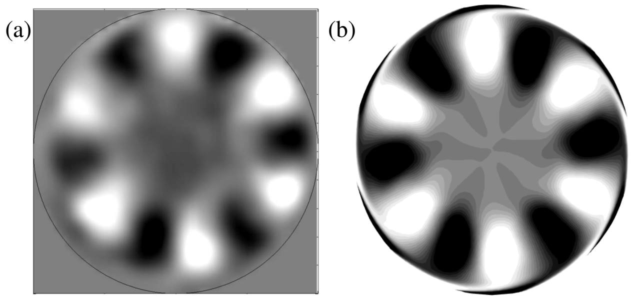

Figure 4: A comparison of contours of axial vorticity extracted at cylinder mid-height when azimuthal modes $m = 5$ and 6 are active. (a): experiment [6], (b): DNS. The only structure visible at this location is for azimuthal wavenumber $m = 6$, in agreement with predictions of weakly nonlinear theory [6].

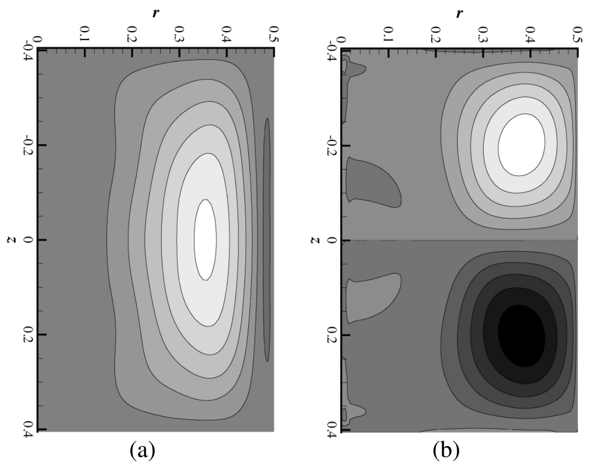

Figure 5: Contours of axial velocity in the meridional semiplane for (a) $m = 5$, (b) $m = 6$.

predicts that at this mid-height location, axial vorticity should only appear for $m = 6$, in good agreement with both experiment and DNS.

Weakly nonlinear theory also predicts that the axial structure of the axial velocity component for the (inviscid) Kelvin modes involved in the coupling should have one half-wavelength $m = 5$ and two for $m = 6$. Figure 5 shows contours of axial velocity component in the meridional semiplane for the (real part of) Fourier mode $m = 5$ and the (imaginary part of) Fourier mode $m = 6$. The observed axial parities and boundary conditions (no-slip) imply that to a good degree of approximation, the axial velocity matches the prediction at each radial location. The presence of only a single dominant maximum in the radial structure of each mode also agrees with the nonlinear theory for the resonance condition for which the problem is tuned.

Figure 6, for $t \approx 340T$, illustrates an overturning flow inside the cylinder. This feature has been noted in previous experiments, e.g. Manasseh (1992) [9]. At this stage it is not completely clear if this overturning is directly connected to the instability.

Figure 7 shows details of the temporal evolution of Fourier-modal kinetic energies in modes $m = 1$ and 5 during the last long-timescale oscillation shown in figure 3. The key new feature here is the temporal evolution of the disturbance azimuthal flow $\overline{w}$, which is the integral over the meridional semi-plane of swirl velocity component obtained after the background solid-

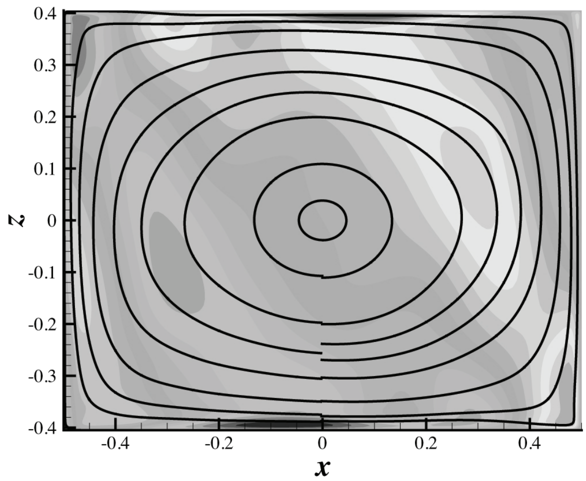

Figure 6: Instantaneous sectional streamlines with contours of out-of-plane velocity in a plane orthogonal to the tilt direction.

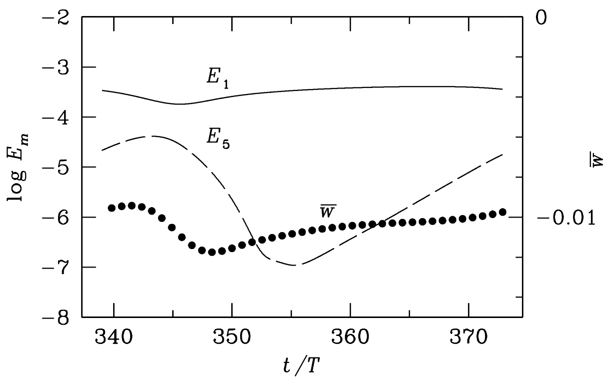

Figure 7: Detail showing kinetic energies at azimuthal wavenumbers $m = 1$ and 5, together with normalised disturbance azimuthal flow rate $\overline{w}$.

body rotation has been subtracted, normalised by the outer wall speed $\Omega_1 R$. Unlike the modal energies, $\overline{w}$ is shown on a linear scale, and note that it is negative, i.e. retrograde. The fact that this disturbance flow varies by only of order 10% from its mean value over the large-scale period while the energy E_5 varies by over two orders of magnitude and E_1 by only about a factor of two, suggests that the azimuthal flow is most strongly coupled to $m = 1$. We note that according to both our related programme of experimental measurement [1] and further simulations conducted at lower Reynolds number, the azimuthal mean flow ('geostrophic flow') arises even in the absence of instability.

Effect of nutation angle variation

For the chosen geometry and rotational speeds, we can vary nutation angle θ, which appears in the weakly nonlinear theory [7] through the Rossby number. The theory (and experiments) suggests that there exists a critical Rossby number below which no instability exists, though of course some energy must exist in all non-zero azimuthal Fourier modes when $\theta > 0$.

In order to study this aspect we have varied nutation angle over the range $0.2^\circ \leq \theta \leq 1.1^\circ$. The outcomes are summarized in figure 8, which shows kinetic energy at $m = 5$ in the long-time limit. The minimum recorded angle for which significant

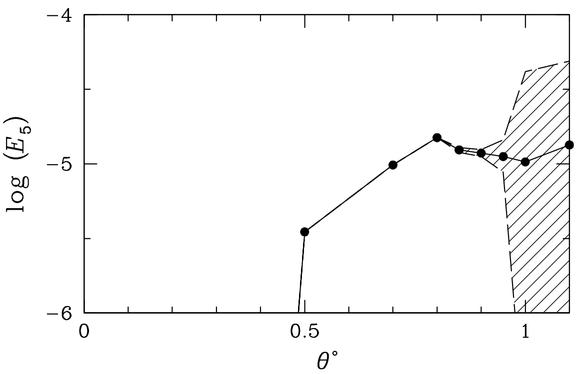

Figure 8: Long-time kinetic energy in azimuthal wavenumber $m = 5$ as a function of nutation angle at $Re = 6500$. Solid line and dots shows mean value, dashed/shaded region shows envelope.

energy existed in $m = 5$ was $\theta = 0.5^\circ$, the maximum steady value occurred for $\theta = 0.8^\circ$, with increasingly significant oscillations appearing for $\theta > 0.8^\circ$, as may be observed e.g. in figures 3 and 7. Thus the minimum recorded Rossby number for which instability was observed in the numerical work to date is $Ro = \Omega_2 \sin(0.5^\circ) = -0.0017$, in good agreement with both theory and experiment [7, Fig. 10].

Conclusions

Our numerical study of the experiments of Lagrange *et al.* [6] has given good support to the weakly nonlinear theory cited in that work and detailed in later references [7, 13], and also helps serve to validate our numerical method which will form the basis for further work to deal with the mechanics of catastrophic collapse. That work will be supplemented by an allied programme of experimental measurements, also described in the present volume [1].

Acknowledgements

We would like to acknowledge financial support from the Australian Research Council through Discovery Program Grant DP130101744, and from Australia's National Computational Infrastructure via Merit Allocation Scheme Grant D77.

References

[1] Albrecht, T., Meunier, P., Mannaseh, R., Lopez, J. M. and Blackburn, H. M., PIV of a precessing cylinder flow, in *Proc. 19th A/Asian Fluid Mech. Conf.*, Melbourne, 2014.

[2] Blackburn, H. M. and Sherwin, S. J., Formulation of a Galerkin spectral element–Fourier method for three-dimensional incompressible flows in cylindrical geometries, *J. Comput. Phys.*, **197**, 2004, 759–778.

[3] Fultz, D., A note on ovestability and the elastoid-inertia oscillations of Kelvin, Solberg, and Bjerknes, *Meteorology*, **16**, 1959, 199–208.

[4] Kelvin, L., Vibrations of a columnar vortex, *Phil. Mag.*, **10**, 1880, 155–168.

[5] Kobine, J. J., Inertial wave dynamics in a rotating precsssing cylinder, *J. Fluid Mech.*, **303**, 1995, 233–252.

[6] Lagrange, R., Eloy, C., Nadal, F. and Meunier, P., Instability of fluid inside a precessing cylinder, *Phys. Fluids*, **20**, 2008, 081701–1–4.

[7] Lagrange, R., Meunier, P., Nadal, F. and Eloy, C., Precessional instability of a fluid cylinder, *J. Fluid Mech.*, **666**, 2011, 104–145.

[8] Malkus, W. V. R., Precession of the earth as a cause of geomagnetism, *Science*, **160**, 1968, 259–264.

[9] Manasseh, R., Breakdown regimes of inertia waves in a precessing cylinder, *J. Fluid Mech.*, **243**, 1992, 261–296.

[10] Manasseh, R., Nonlinear behaviour of contained inertia waves, *J. Fluid Mech.*, **315**, 1996, 151–173.

[11] McEwan, A. D., Inertial oscillations in a rotating fluid cylinder, *J. Fluid Mech.*, **40**, 1970, 603–640.

[12] McEwan, A. D., Degeneration of resonantly-excited standing internal gravity waves, *J. Fluid Mech.*, **50**, 1971, 431–448.

[13] Meunier, P., Eloy, C., Lagrange, R. and Nadal, F., A rotating fluid cylinder subject to weak precession, *J. Fluid Mech.*, **599**, 2008, 405–440.